

1 **Seasonal cycles in a seaweed holobiont: A multiyear time series reveals**  
2 **repetitive microbial shifts and core taxa**

3  
4 Chantal Marie Mudlaff<sup>1,2</sup>, Florian Weinberger<sup>1</sup>, Luisa Düsedau<sup>1,3</sup>, Marjan Ghotbi<sup>1,2</sup>,  
5 Sven Künzel<sup>4</sup>, Guido Bonthond<sup>1,5</sup>

6  
7 <sup>1</sup> Department of Marine Ecology, GEOMAR Helmholtz Centre for Ocean Research Kiel, 24105  
8 Kiel, Germany

9 <sup>2</sup> Faculty of Mathematics and Natural Sciences, Christian-Albrechts-Universität zu Kiel, 24118  
10 Kiel, Germany

11 <sup>3</sup> Section Benthic Ecology, Alfred Wegener Institute Helmholtz Centre for Polar and Marine  
12 Research, 27570 Bremerhaven, Germany

13 <sup>4</sup> Department of Evolutionary Genetics, Max Planck Institute for Evolutionary Biology, Plön,  
14 Germany

15 <sup>5</sup> Institute for Chemistry and Biology of the Marine Environment (ICBM), School of Mathematics  
16 and Science, Carl von Ossietzky Universität Oldenburg, Ammerländer Heerstraße 114-118,  
17 26129 Oldenburg, Germany

18  
19

20 **ORCID**

21 *Chantal Marie Mudlaff* <https://orcid.org/0009-0004-7789-269X>

22 *Florian Weinberger* <https://orcid.org/0000-0003-3366-6880>

23 *Luisa Düsedau* <https://orcid.org/0000-0002-2750-6437>

24 *Marjan Ghotbi* <https://orcid.org/0000-0003-4655-6445>

25 *Guido Bonthond* <https://orcid.org/0000-0002-9823-6761>

26  
27

28

29 **Keywords:** seasonality, seaweed, macroalga, holobiont, seaweed holobiont, epibiota,  
30 host-microbe

31 **ABSTRACT**

32

33 Seasonality is an important natural feature that drives cyclic environmental changes.  
34 Seaweed holobionts, inhabiting shallow waters such as rocky shores and mud flats, are subject  
35 to seasonal changes in particular, but little is known on the influence of seasonality on their  
36 microbial communities.

37 In this study, we conducted a bi-monthly, three-year time series to assess the seasonality  
38 of microbial epibiota in the seaweed holobiont *Gracilaria vermiculophylla*. Our results reveal  
39 pronounced seasonal shifts that are both taxonomic and functional, oscillating between late  
40 winter and early summer across consecutive years. While epibiota varied taxonomically  
41 between populations, they were functionally similar, indicating that seasonal variability drives  
42 functional changes, while spatial variability is more redundant.

43 We also identified seasonal core microbiota that consistently (re)associated with the host  
44 at specific times, alongside a permanent core that is present year-round, independent of  
45 season or geography. These findings highlight the dynamic yet resilient nature of seaweed  
46 holobionts and demonstrate that their epibiota undergo predictable changes. Therewith, the  
47 research offers important insights into the temporal dynamics of seaweed-associated  
48 microbiota, and demonstrates that the relationship between seaweed host and its epibiota is  
49 not static, but naturally subject to an ongoing seasonal succession process.

## 50 INTRODUCTION

51  
52 Seasonality is a global environmental feature which plays an important role in structuring  
53 communities in terrestrial and aquatic environments (White & Hastings 2020). To communities,  
54 seasonality is a natural source of variability, characterized by cyclic changes in temperature  
55 and photoperiod, but also by other variables such as salinity, rainfall, phytoplankton blooms,  
56 anthropogenic stressors, upwelling, and nutrient pulses (Lisovski *et al.* 2017). Seasonal  
57 fluctuations are also prevalent in free-living microbial communities (Fuhrman *et al.* 2015;  
58 Gilbert *et al.* 2012) and microbial communities associated with various hosts (Sharp *et al.* 2017;  
59 Ferguson *et al.* 2018; Gobbi *et al.* 2020; Risely *et al.* 2021), including seaweeds (Bengtsson  
60 *et al.* 2010; Park *et al.* 2022; Tujula *et al.* 2010).

61 Seaweeds are typically found in coastal habitats, such as rocky shores and intertidal  
62 mudflats, which experience strong seasonal forces (Benincà *et al.* 2015). Naturally, seaweed  
63 holobionts are surrounded by microbial life. The algal surface is in direct contact with the  
64 surrounding water and acts as substrate on which microorganisms can settle (Wahl *et al.*  
65 2012). These colonizing communities are typically dominated by bacteria, but also include  
66 microalgae, fungi, protists, and viruses (Egan *et al.* 2013; Van Der Loos *et al.* 2019). On the  
67 interface between the seawater and the inner tissue of the seaweed, epibiota form a dynamic  
68 biofilm, which has also been termed the “second skin” and influence the host physiologically,  
69 chemically and biologically (Wahl *et al.* 2012). These epibiota include (opportunistic)  
70 pathogens, but also beneficial microbes that promote the host’s development and fitness, such  
71 as e.g., sporulation (Weinberger *et al.* 2007) or morphogenesis (Weiss *et al.* 2017, reviewed  
72 in Egan *et al.* 2013), pathogen recognition, and chemically mediated defense mechanisms (Li  
73 *et al.* 2022; Longford *et al.* 2019; Rao *et al.* 2007; Saha & Weinberger 2019).

74 Epiphytic communities are complex and their structure depends on host morphology  
75 (Lemay *et al.* 2021), varies by species (Lachnit *et al.* 2009, 2011) or even lifecycle stage  
76 (Lemay *et al.* 2018; Bonthond *et al.* 2022), and differs along the algal thallus (Paix *et al.* 2020),  
77 implicating the specific and diverse niches provided by the host and the microbial partners.  
78 The holobiont is exposed to variable environmental conditions, which may alter the epibiota  
79 composition either directly, or indirectly via host physiological responses to the changing  
80 environment. For instance, seaweed epibiota have been found to strongly vary with salinity  
81 (Stratil *et al.* 2014; Van Der Loos *et al.* 2023) and temperature (Stratil *et al.* 2013; Bonthond *et al.*  
82 2023). Thus, seaweed epibiota are shaped by a combination of host and environment. As  
83 both environmental conditions and host physiology are seasonal, it is not surprising that  
84 seasonal patterns have been detected in seaweed epibiota (Bengtsson *et al.* 2010; Park *et al.*  
85 2022; Tujula *et al.* 2010). While it is informative to document microbial changes within the  
86 holobiont from one season to another, it is important to distinguish which changes are  
87 repetitive. Such cyclic patterns reflect an ongoing interaction between host and microbiota,  
88 with long multigenerational histories. Microbial taxa that are present irrespective of season, or  
89 that return interannually, may represent important core symbionts (beneficial or harmful).  
90 Studying holobionts during different seasons across several years may resolve such  
91 permanent and/or seasonal core microbiota and therewith contribute to the identification of  
92 important host-microbe associations and to better understand the complex dynamics within  
93 the holobiont.

94 *Gracilaria vermiculophylla* is a well-studied holobiont. This perennial rhodophyte is native  
95 to the North-West Pacific (Kim *et al.* 2010; Krueger-Hadfield *et al.* 2017, 2021) but has become  
96 invasive across the Northern Hemisphere, including the Eastern Pacific southward to Mexico  
97 (Bellorin *et al.* 2004), the North American coasts in the Western Atlantic (Freshwater *et al.*  
98 2006; Thomsen *et al.* 2006), as well as the European coasts at the Eastern Atlantic, extending

99 towards northern parts of the North Sea and the South Western Baltic Sea (Rueness 2005;  
100 Thomsen 2007; Weinberger *et al.* 2008). Epibiota associated with *G. vermiculophylla* have  
101 been studied across the Northern Hemisphere (Bonthond *et al.* 2020), which revealed that  
102 some epi- and endobiota were part of a core, i.e., a group of microbial taxa that was associated  
103 with the *G. vermiculophylla* holobiont irrespective of the host geography. This holobiont was  
104 also studied in controlled experiments in the lab, and its microbiota were sampled repeatedly  
105 over several weeks to months (Bonthond *et al.* 2021a, 2023). These time series demonstrated  
106 that epi- and endobiota within the holobiont have strong temporal variation and that not all  
107 geographic core microbiota were temporally stable. Altogether, this may indicate that many  
108 core microbes are rather season specific. Given the wide geographic stretch, across which  
109 spatial variability and core microbes have already been studied in Bonthond *et al.* (2020),  
110 *G. vermiculophylla* presents a suitable seaweed holobiont to characterize seasonal variability  
111 and core microbiota.

112 The aim of the present study was therefore to evaluate seasonal variability in  
113 *G. vermiculophylla* associated epibiota as well as to characterize cyclic patterns and  
114 permanent core microbiota (i.e., seasonal and interannual). To this end, we conducted a bi-  
115 monthly time series sampling of *G. vermiculophylla* individuals from two distinct populations  
116 over three consecutive years, resulting in a dataset with 18 repeated measures. We  
117 hypothesized that prokaryotic epibiota associated with *G. vermiculophylla* show seasonality,  
118 in terms of taxonomic and functional composition and in terms of diversity. Furthermore, we  
119 hypothesized that *G. vermiculophylla* harbors core microbiota, which are (i) permanent (i.e.,  
120 associated irrespective of time and space) as well as (ii) season-specific (i.e., consistently  
121 present in the holobiont during specific times of the year).

122  
123  
124

## 125 **EXPERIMENTAL PROCEDURES**

126

### 127 *Sample collection*

128 Seaweeds were collected in Nordstrand (Germany) at the North Sea (54°29'9.34"N  
129 8°48'44.65"E) and in Heiligenhafen (Germany) at the Baltic Sea (54°22'46.7"N 10°58'57.5"E;  
130 Fig. 1A-D). These populations were chosen based on their distinct environmental features.  
131 The North Sea population is found in the intertidal zone. Here, the perennial  
132 *Gracilaria vermiculophylla* occurs mainly attached to hard substratum and can build massive  
133 mats during spring and/or summer. In contrast, the Baltic Sea population is situated in a small  
134 lagoon sheltered from turbulences and is only experiencing wind driven sea level fluctuations.  
135 Here, the *G. vermiculophylla* individuals are not attached to substratum but rather loosely  
136 embedded in the soft sediment. During winter, the number of individuals typically reduces  
137 substantially and sometimes appears to be absent. Whereas individuals in the North Sea  
138 population are exposed to fully marine salinities (i.e., ~ 24 to 32, Fig. 1E) and diurnal air  
139 exposure, the Baltic Sea population experiences rather brackish salinities (between ~ 10 and  
140 20, Fig. 1E) as well as less and irregular air exposure. Generally, the pH is more similar  
141 between the two populations, normally fluctuating between 7 and 9, although an outlier was  
142 detected in Heiligenhafen of 5.3, recorded during early summer in year 1 (Fig. 1F).

143 The sample collection took place in bi-monthly intervals covering a three-year time period  
144 from February 2018 to January 2021. During these years water temperatures at locations  
145 nearby to Nordstrand and Heiligenhafen oscillated similarly between minima of 1 to 6°C in  
146 winter and maxima of 21 to 23°C in summer (Fig. 1G). At each sampling point,  
147 10 *G. vermiculophylla* individuals were collected with gloves and placed separately into plastic  
148 bags. To avoid collection of the same individual, the individuals were sampled at least 1 m  
149 away from each other. In the North Sea population, only attached algae were sampled.  
150 Additionally, three 50 ml water and two 15 ml sediment samples were taken at both sites.  
151 Subsequently, around 0.25 ml sediment was transferred into a 2 ml tube containing absolute  
152 ethanol. After collection, all samples were transported in a cooling box back to the facilities of  
153 GEOMAR Helmholtz Centre for Ocean Research in Kiel (Germany) where they were stored at  
154 4°C and processed within two days maximum. In the laboratory, salinity and pH were  
155 measured for both collection sites from one of the three water samples. The remaining water  
156 samples were processed further together with the seaweed samples.

157

### 158 *Generating epiphytic extracts*

159 To generate extracts from the prokaryotic epibiota associated with *G. vermiculophylla*, the  
160 method in Bonthond *et al.* (2020) was followed. In brief, a branch of  $1 \pm 0.25$  g was transferred  
161 into a 50 ml tube. Approximately 10 glass beads and 15 ml artificial seawater of the respective  
162 salinity (prepared from distilled water and sodium chloride) were added. Besides the field  
163 samples, at least one blank was prepared for each sampling event, containing only glass beads  
164 and distilled water. Afterwards, all samples were vortexed for 2 min at maximum rotation  
165 speed. After vortexing, the algal tissue was removed. For the samples collected in the first  
166 sampling year, the epiphytic suspension was filtered as in Bonthond *et al.* (2020). During the  
167 second and third year, the centrifugation method of Ficetola *et al.* (2008) was used. In brief,  
168 33 ml absolute ethanol and 1.5 ml sodium acetate were added to 15 ml epiphytic suspension,  
169 water, and blank samples. All tubes were mixed and either processed immediately or cooled  
170 at 4°C and processed in the next days. The 50 ml tubes were then centrifuged for 10 min at  
171 14,000 g. The supernatant was discarded and the pellet was preserved in 1 ml absolute

172 ethanol. The generated epiphytic algal extracts (on filters or in 1 ml ethanol), water, sediment,  
173 and blanks were stored at – 20°C until DNA extraction.

174

#### 175 *DNA extraction & amplicon library preparation*

176 Ethanol was removed from the samples by evaporation in a vacuum centrifuge for at least  
177 1 hour at 45°C. If the evaporation of the alcohol was unsuccessful after several hours, the  
178 remaining ethanol was removed by lyophilization. Filters were fragmented to small pieces with  
179 sterile scissors. Subsequently, DNA was extracted following the Cetyltrimethylammonium  
180 bromide (CTAB)–chloroform protocol from Doyle & Doyle (1987). The amplicon library was  
181 prepared following a two-step PCR approach by Gohl *et al.* (2016), using the same indexing  
182 primers and KAPA HIFI HotStart polymerase (Roche). The first PCR targeted the V4 region of  
183 the 16S rRNA gene using the forward primer U515F (S\*-Univ-0515-a-S-19) and the reverse  
184 primer 806R (S-D-Arch-0786-a-A-20; Klindworth *et al.* 2013) with adapters for the second PCR  
185 on 5' ends. The first PCR program began with a step of 5 min at 95°C and was followed by  
186 25 cycles of denaturation for 20 sec at 98°C, annealing for 15 sec at 55°C, and elongation for  
187 1 min at 72°C. For water samples which were not successfully amplified, 30 cycles were used  
188 in a repeated PCR attempt.

189 For the second PCR, the amplicon products were diluted 1:10 and used as template. PCR  
190 was conducted following the same cycling program, but with 10 cycles of denaturation and an  
191 additional final elongation step of 10 min at 72°C. Subsequently, PCR products were visualized  
192 by gel electrophoresis and relative amplicon concentrations were estimated from gel pictures  
193 using the software Image J Fiji (Fiji for Mac OS X Version 1.0) to accordingly adjust volumes  
194 in the library pooling. The pooled library was purified with a gel extraction step by using the  
195 ZymoClean Gel DNA recovery kit (ZymoResearch) following the supplied protocol, quantified  
196 with qPCR, and sequenced as paired-end reads (2 x 300) on the Illumina MiSeq platform at  
197 the Max Planck Institute in Plön (Germany).

198

#### 199 *Data processing*

200 A total of 406 samples (including controls) was processed with the software Mothur  
201 (v.1.43.0 and v.1.45.3; Schloss *et al.* 2009) following an inhouse script. Accordingly, unique  
202 sequences were aligned to and classified with the SILVA reference alignment v132 (Quast *et al.*  
203 *et al.* 2013). The sequences were open-reference clustered to the 3% OTUs from a field study  
204 by Bonthond *et al.* (2020) with the *cluster.fit()* function (Sovacool *et al.* 2022). Sequences of  
205 mitochondrial, chloroplast, eukaryotic, and unknown origin were removed. Finally, OTUs that  
206 were singletons in the full dataset and samples with < 1000 reads were removed. The raw  
207 demultiplexed amplicon reads were deposited in the SRA database (accession:  
208 PRJNA1155875). Predicted metagenomes based on KEGG Ortholog (KO) annotations  
209 (Kanehisa *et al.* 2014) were obtained with PICRUST2 v2.5.0 (Douglas *et al.* 2020).

210 The variability in the taxonomic (based on OTUs) and functional (based on predicted KOs)  
211 community composition over time was visualized with non-metric multidimensional plots  
212 (nMDS) using Bray-Curtis distances with the R package vegan (Oksanen 2010), based on  
213 rarefied data of either all samples including all substrates (alga, water, and sediment) or solely  
214 algal substrates only. Additionally, trajectories were drawn chronologically through the group  
215 centroids of algal samples from the same sampling event. To test for differences in taxonomic  
216 and potential functional community composition, permutational multivariate analysis of  
217 variance (PERMANOVA) was applied on the unrarefied OTU data set, by using 9,999  
218 permutations in the R package vegan (Oksanen 2010; usage of the *adonis2* function). First, a  
219 PERMANOVA was run on the full OTU and KO datasets, including alga, water, and sediment

220 samples. The model included the variables season (as factor with 6 levels), year (as factor  
221 with 3 levels), population (as factor with 2 levels), substrate (alga, water, and sediment), and  
222 all interactions. Subsequently, a PERMANOVA was run on the OTU and KO datasets of only  
223 algal samples, with the variables season, year, population, and all possible interactions. In  
224 both PERMANOVAs, the sequencing depth was logarithmic transformed (LSD) and included  
225 as covariate to account for its effect.

226 To analyze the microbial diversity the asymptotic species richness ( $S_{\text{Chao}}$ ) was calculated  
227 with the R package iNEXT v3.0.0 (Chao *et al.* 2014; Hsieh *et al.* 2016). Second, as a measure  
228 of evenness, the probability of interspecific encounter (PIE; Hurlbert 1971), was calculated with  
229 the R package mobr v2.0.2 (McGlenn *et al.* 2019). For both diversity measures the total data  
230 set containing exclusively algal OTU read counts was used. For the  $S_{\text{Chao}}$ , a generalized linear  
231 model (GLM) was fitted, including the main effects of season (as factor with 6 levels,  
232 corresponding to the sampling events repeated over three years), year (as factor with 3 levels),  
233 population (as factor with 2 levels), and all possible interactions. The model assumed a  
234 gaussian family distribution, with a logarithm in the link function. The log transformed  
235 sequencing depth (LSD) was included as a covariate to account for variation in total read  
236 counts across samples. For the PIE, a GLM with the same model structure was used. PIE was  
237 logit transformed to meet the model assumptions. As the sequencing depth was not significant,  
238 it was excluded from the model. Analysis of variance (ANOVA) was applied to the GLM of  $S_{\text{Chao}}$   
239 and PIE to test for significance. If the main effects season, year, and population were  
240 significant, post-hoc analysis was performed by pair-wise comparisons in both models on all  
241 possible interactions between the main effects by using the R package emmeans v1.8.9 (Lenth  
242 2022).

#### 243 244 *Defining permanent and seasonal core microbiota*

245 Core microbiota were identified using two alternative compositional approaches by  
246 identifying differentially abundant OTUs (see Shade & Handelsman 2012 for definitions on  
247 core microbiomes). With both approaches we defined both a permanent core, including OTUs  
248 persistently detected within the epibiota across all seasons and years, and two seasonal cores,  
249 including OTUs consistently detected within either summer or winter.

250 The first approach was based on multivariate GLMs (mGLMs) from the R package mvabund  
251 v4.2.1 (Wang *et al.* 2012), which was also used to characterize the spatial core in Bonthond *et al.*  
252 (2020). mGLMs were fitted on the cumulative 95% most abundant OTUs with > 25%  
253 prevalence and assumed a negative binomial distribution. For the permanent core, the  
254 variables substrate (alga, water or sediment), season (6 levels, t1:t6) and year (3 levels) were  
255 included as predictors. For seasonal mGLM cores, the OTU matrix was reduced to season  
256 time points t1 (late winter), t3 (early summer), t4 (late summer) and t6 (early winter) and the  
257 factor 'season' was reduced to only two levels representing the seasonal extremes (winter: t6  
258 & t1, summer: t3 & t4), and included in the model together with the factor year. Both mGLMs  
259 included the LSD as offset to correct for different sequencing depths across samples. Models  
260 were resampled using the summary.manyglm function with 500 bootstrap iterations, which  
261 were restricted within populations. The p-values were obtained through Wald tests. OTUs were  
262 considered part of the permanent core when the coefficients  $\text{substrate}_{\text{alga:water}}$  and  
263  $\text{substrate}_{\text{alga:sediment}}$  were negative (reflecting higher relative OTU abundances associated with  
264 algal samples compared to water and sediment) and with corresponding p-values < 0.01.  
265 Similarly, OTUs with positive and negative coefficients for the factor  $\text{season}_{\text{summer:winter}}$  and with  
266 p-values < 0.01, were considered winter and summer core OTUs, respectively.

267 In addition to the mGLM core, we also defined a compositional core with the linear  
268 discriminant analysis effect size method (LEfSe, Segata *et al.* 2011) through the online  
269 interface at the webpage from the Huttenhower lab  
270 (<https://huttenhower.sph.harvard.edu/galaxy/>; accessed May 2023). For the permanent LEfSe  
271 core, OTUs significantly more abundant in epibiota samples compared to both water and  
272 sediment samples were considered core OTUs. Also, for seasonal LEfSe cores, the dataset  
273 was reduced to summer (time points t3 and t4 combined) and winter (time points t1 and t6  
274 combined) to identify OTUs significantly more abundant in either season.

275  
276

## 277 RESULTS

278

### 279 Sequencing summary

280 After all quality filtration steps, the final dataset counted 262 samples (170 algal, 29 water,  
281 and 63 sediment samples) and 14,874,961 sequencing reads, clustered into 45,751 OTUs,  
282 including 17,670 OTUs that were already identified in Bonthond *et al.* (2021). The overall most  
283 abundant OTU in the holobiont was classified to *Granulosicoccus* (OTU97) with a mean  
284 relative abundance of 4.93% and 99.4% occupancy, followed by OTUs classified to  
285 Alphaproteobacteria (OTU12, 1.82% abundance and 100% occupancy), Rhodobacteraceae  
286 (OTU00003, 1.73% relative abundance and 100% occupancy), and *Desulforhopalus*  
287 (OTU1577, 1.51% relative abundance and 91.60% occupancy). The most abundant families  
288 were Rhodobacteraceae (18.17%), Flavobacteriaceae (15.13%), Saprospiraceae (10.73%)  
289 and Thiohalorhabdaceae (4.81%, Fig. 2).

290

291 The collected prokaryotic surface communities associated to the red seaweed  
292 *Gracilaria vermiculophylla* compositionally differed from the seawater and sediment  
293 communities. Although the classes Gammaproteobacteria, Alphaproteobacteria, Bacteroidia,  
294 and Deltaproteobacteria contributed to the general community composition structure and were  
295 shared between all three substrates, detectable differences in abundance occurred already in  
296 the top 10 families (Fig. S1). Notably, the ten most abundant prokaryotic families contributed  
297 around 65% of all families present on *G. vermiculophylla*, but less than 50% of those present  
298 in sediment and water. The families Flavobacteriaceae and Rhodobacteraceae were  
299 particularly important in algal and seawater samples, while Halieaceae, Desulfobulbaceae,  
300 Desulfobacteraceae, Chromatiaceae, and Pirellulaceae were more important in sediment  
301 samples. Interestingly, Thiohalorhabdaceae, Thiotrichaceae, Sphingomonadaceae, and  
302 Pseudoalteromonadaceae only occurred in the top 10 families of algal samples (Fig. S1).

303 Microbiota on algal surfaces varied considerably over time. Regarded for both populations  
304 together and throughout the years, Gammaproteobacteria were mainly represented by  
305 Thiohalorhabdaceae, Alphaproteobacteria by Rhodobacteraceae, and Bacteroidia by  
306 Flavobacteriaceae and Saprospiraceae. This pattern was best visible in the second and third  
307 year (Fig. 2). Additionally, each year had a specific pattern of interchanging families along  
308 seasons. Desulfobulbaceae tended to be less prominent in summer than in winter, while an  
309 opposite pattern was observed for Rhizobiaceae (Fig. 2). However, exceptions occurred. For  
310 instance, Rhizobiaceae were also relatively abundant in winter (t6) in the third year and an  
311 exceedingly high abundance of Pseudoalteromonadaceae was once observed at t1 in the  
312 beginning of the first year.



313 Microbiota on algal surfaces also varied between the populations (Fig. S2).  
314 Thiohalorhabdaceae, Thiotrichaceae, Microtrichaceae, and Rhizobiaceae solely occurred in  
315 the ten most abundant families at Nordstrand, whereas dominant families associated primarily  
316 to Heiligenhafen were Pseudoalteromonadaceae, Sphingomonadaceae, Cellvibrionaceae,  
317 and Pirellulaceae. A comparison of community compositions at the two populations over time  
318 (Fig. S3) generally confirmed these differences, as well as the pertaining dominance of a small  
319 group of families within each population. At the same time, the clear dominance of certain  
320 microbial families at specific seasons mainly disappeared and a more fine-tuned picture  
321 established. More families appeared within the top 10, which often exhibited more fluctuating  
322 abundances throughout the year. Families that emerged predominantly in Nordstrand were for  
323 instance Bdellovibrionaceae and JGI\_0000069-P22\_fa (Gracilibacteria). In contrast, new  
324 families belonging to the Oxyphotobacteria appeared in Heiligenhafen among the top 10  
325 mainly in summer (t3) and beginning of autumn (t4) throughout the first two years (Fig. S3).

### 326 327 *Community composition*

328 An nMDS based on taxonomic composition clearly separated algal samples and sediment  
329 samples, while seawater samples arranged amid those two (Fig. S4). A PERMANOVA  
330 confirmed that much compositional variation was explained by the substrate ( $R^2 = 0.117$ ;  
331  $p < 0.001$ , Table S1). Among algal samples only, another significant source of differences in  
332 microbial taxonomic composition was the population (PERMANOVA,  $R^2 = 0.053$ ;  $p < 0.001$ ,  
333 Table S1; for algal samples only  $R^2 = 0.109$ ;  $p < 0.001$ ; Table S2). nMDS correspondingly  
334 separated samples collected from algal surfaces and sediment samples at Nordstrand and  
335 Heiligenhafen nearly completely, while water samples exhibited more compositional similarity  
336 between populations (Fig. S4).

337 Microbial taxonomic community composition varied significantly over time. Season and year  
338 together (individually or in interaction with other factors) explained much of the compositional  
339 differences between samples (PERMANOVA, Table S1 for all samples and Table S2 for algal  
340 samples only). nMDS indicated that the taxonomic composition of epiphytic communities  
341 varied by season, with similar seasonal shifts across years (Fig. 3A). Correspondingly,  
342 PERMANOVA confirmed that the clustering by season ( $R^2 = 0.092$ ;  $p < 0.001$ ; Table S2, Fig.  
343 3B) was stronger than clustering by year ( $R^2 = 0.028$ ;  $p < 0.001$ ; Table S2). Despite substantial  
344 differences between the two populations ( $R^2 = 0.109$ ;  $p < 0.001$ ) the seasonal shifts in microbial  
345 composition were similar in direction and magnitude.

346 While functional community composition was also strongly shaped by season ( $R^2 = 0.092$ ;  
347  $p < 0.001$ ), differences between populations were limited ( $R^2 = 0.007$ ,  $p = 0.041$ ) and not clearly  
348 visible in the nMDS, although functions are derived from taxonomy. Also, the factor year  
349 explained more functional diversity ( $R^2 = 0.016$ ;  $p = 0.008$ ) than the factor population, which  
350 was not the case for taxonomic diversity (Tables S2 and S3). nMDS confirmed that functional  
351 diversity oscillated between summer and winter (Fig. 3C)

### 352 353 *Diversity*

354 The asymptotic OTU Chao richness ( $S_{\text{Chao}}$ ) of microbial communities on the surface of  
355 *G. vermiculophylla* showed significant seasonal variation (Likelihood Ratio  $\chi^2(5) = 59.076$ ,  
356  $p < 0.001$ ; Table S4). It was characterized by a minimum in early summer (t3) and a maximum  
357 in late winter (t1) and was rather constant from summer (t4) to early winter (t6) (Fig. 4A; Table  
358 S4). A different seasonal pattern emerged for evenness (Likelihood Ratio  $\chi^2(5) = 86.574$ ,  $p <$   
359  $0.001$ ; Table S5). PIE was highest in summer (t4) and minimal during winter (t6 and t1, Fig.

360 4B). Similar to Chao richness in OTUs, Chao richness of predicted functions showed strong  
361 seasonal variation (Likelihood Ratio  $\chi^2(5) = 34.03$ ,  $p < 0.001$ ; Table S4) with a maximum in  
362 late winter (t1) and minimum in early summer (t3), but transitioned more gradually towards  
363 these extremes over the other seasonal time points (Fig. 4C, Table S4). Evenness in predicted  
364 functions varied with season as well (Likelihood Ratio  $\chi^2(5) = 39.519$ ,  $p < 0.001$ ; Table S5), but  
365 yielded a more complex trend with multiple optima (t4, t6) and minima (t2, t3, t5, Fig. 4D, Table  
366 S5).

### 367 368 *Core microbiota*

369 Linear discriminant analysis identified several taxa as permanent biomarkers of  
370 *G. vermiculophylla* surfaces, i.e. they were at all times of the year significantly less  
371 characteristic for sediment and water samples (Fig. 5A, Table S6-7). The approach identified  
372 8 OTUs that formed a permanent LEfSe-core of the algal host (Fig. 5A, Table S6), and also  
373 several higher taxonomic ranks as LEfSe-core groups (Table S7), including the phylum  
374 Bacteroidetes, the classes Alphaproteobacteria and Bacteroidia, four different orders (highest  
375 LDA score: Flavobacteriales), nine different families (highest LDA scores: Flavobacteriaceae  
376 and Hyphomonadaceae), and 12 different genera (Highest LDA score: *Granulosicoccus*).  
377 Altogether 69 OTUs formed a summer LEfSe-core of *G. vermiculophylla* and 33 OTUs formed  
378 a winter LEfSe core (Fig. 5B-C, Table S6). Biomarkers of summer (Fig. 5B, Table S7) were  
379 the dominant bacteria, the class Alphaproteobacteria, six orders (highest LDA scores:  
380 Rhodobacterales and Chitinophagales), eight families (highest LDA scores:  
381 Rhodobacteraceae and Saprospiraceae) and eight genera (highest LDA score: *Ulviabacter*).  
382 Taxonomic biomarkers of the winter season (Fig. 5C, Table S7) were the phyla Proteobacteria  
383 and Firmicutes, the class Clostridia, three orders (highest LDA score: Thiotrichales), six  
384 families (highest LDA score: Desulfobulbaceae) and 12 genera (highest LDA score:  
385 *Desulforhopalus*).

386 The permanent and seasonal cores defined by the mGLM approach overlapped to some  
387 extent with the cores characterized by the linear discriminant analysis. The permanent mGLM-  
388 core counted 88 OTUs (Fig. 5D for the 25 most abundant OTUs, Table S6). 5 of the 8 OTUs  
389 LEfSe-core OTUs were also identified as part of the mGLM-core (Table S6). The summer  
390 mGLM-core of *G. vermiculophylla* counted 205 OTUs (Fig. 5E for the 25 most abundant OTUs,  
391 Table S6). 50 of the 69 the LEfSe summer core OTUs were also part of the summer mGLM-  
392 core. The mGLM winter core counted 285 OTUs. 21 out of the 33 LEfSe winter core OTUs  
393 were also part of the winter mGLM-core (Fig. 5F for the 25 most abundant OTUs, Table S6).

## 394 395 396 **DISCUSSION**

397  
398 This study revealed that epibiota associated with the seaweed holobiont *Gracilaria*  
399 *vermiculophylla* show strong seasonality. Prokaryotic composition and diversity are highly  
400 variable throughout the year. This variation was largely cyclic, showing similar trends over the  
401 three repetitive years in this study, with late winter and early summer as the extremes between  
402 which composition and diversity oscillated (Fig. 3-4). Our data also indicate that these seasonal  
403 shifts are not functionally redundant, as concurrent trends were found in terms of composition  
404 and diversity of predicted functions. Therewith, these findings support our hypothesis that the  
405 *G. vermiculophylla* holobiont has seasonal dynamics, providing evidence that seaweed  
406 associated epibiota undergo seasonal successional cycles. In line with this, we found  
407 numerous seasonal core taxa, that is, microbial OTUs or groups of higher taxonomic ranks,

408 that were consistently associated with either summer or winter. In addition, our study also  
409 identified a permanent core, of microbial taxa which were consistently associated with the host  
410 independent of season.

#### 411 412 *Temporal variation in epibiota is highly seasonal*

413 Seasonal patterns have been described in seaweeds before, including chemical host  
414 processes such as metabolite production (Paix *et al.* 2019) or anti-fouling activity (Saha & Wahl  
415 2013; Wang *et al.* 2018). Also in microbial communities associated with seaweeds, variability  
416 associated with seasonal changes has been observed (Bengtsson *et al.* 2010; Burgunter-  
417 Delamare *et al.* 2023; Korlević *et al.* 2021; Lachnit *et al.* 2011; Mancuso *et al.* 2016; Park *et al.*  
418 2022; Tujula *et al.* 2010). However, while covering different seasons, the sampling in these  
419 studies is typically limited to one year (with the exception of Lachnit *et al.* 2011). Our findings  
420 are strongly in line with their observations, showing that also in the *G. vermiculophylla*  
421 holobiont, composition and diversity shift from one season to another. By repeating the  
422 seasonal sampling across three subsequent years, our study also resolves interannual trends  
423 which demonstrate that much of this temporal variation is repetitive and therefore truly  
424 seasonal (Fuhrman *et al.* 2015). Epibiota associated with *G. vermiculophylla*, are thus highly  
425 dynamic, but also resilient, as they undergo strong compositional shifts, but shift back towards  
426 compositions experienced in preceding years, in the same season.

427 Given the known structuring effects of both salinity (Stratil *et al.* 2014; Van Der Loos *et al.*  
428 2023) and temperature on seaweed associated microbiota (Bonthond *et al.* 2023; Düsedau *et al.*  
429 2023; Stratil *et al.* 2013), such seasonal environmental variables may well explain much of  
430 the here observed cyclic compositional and diversity changes. At the same time, they may also  
431 explain the pronounced differences in taxonomic composition that were observed between two  
432 sampling sites in the present study. However, besides the environment, also the host  
433 undergoes metabolic, physiological, and reproductive changes which can be season  
434 dependent (Liu *et al.* 2017 and references therein). Cycles in the host can also coincide with  
435 microbial life cycles, such as for example in the brown alga *Ascophyllum nodosum*, whose  
436 reproductive cycles are synchronized with the fungal symbiont *Stigmatidium ascophylli* (Stanley  
437 1992) or in *Acrochaetium* (Rhodophyta), in which bacterial metabolites (N-acyl-homoserine-  
438 lactones) regulate spore release (Weinberger *et al.* 2007). In this context, an interesting  
439 observation is that functional and taxonomic composition of the bacterial communities  
440 associated with *G. vermiculophylla* oscillated seasonally with similar intensity, whereas  
441 pronounced taxonomic differences between sites were hardly reflected by similar functional  
442 differences. Different *G. vermiculophylla* epibiota appear to be functionally similar between  
443 sites in a given season, but are functionally different among seasons. This suggests that the  
444 holobiont acquired season specific microbial functions, but is rather promiscuous to the  
445 microbes that provide them.

#### 446 447 *Seasonal shifts in diversity*

448 The shift from an OTU richness maximum in late winter to a minimum in summer (Fig. 4A),  
449 as well as an inverse pattern of evenness (Fig. 4B) was consistent across both populations  
450 and showed similarity to a study on temporal dynamics on the epibiota associated with the  
451 brown seaweed *Cystoseira compressa* (Mancuso *et al.* 2016). Moreover, this cyclic trend in  
452 Chao richness appeared to be even stronger in terms of predicted functions, which implies that  
453 seasonal changes in diversity are not functionally redundant, resulting in more diverse  
454 functions in winter in the associated epibiota. Hypothetically, a decrease in taxonomic and  
455 functional richness toward summer may be driven by rising temperatures and solar irradiance,

456 with which metabolic rates increase (Clarke & Fraser 2004; Gillooly *et al.* 2001), and reinforce  
457 competition and extinction rates within the seaweed microbiota. If this is true, the seasonal  
458 diversity cycle in *G. vermiculophylla* may be a more general trend among seaweed holobionts.  
459 However, due to limited studies on seaweed holobionts including both seasonal and  
460 interannual samplings this remains to be evaluated in future studies, targeting different  
461 seaweeds.

462

#### 463 *The core microbiome of Gracilaria vermiculophylla*

464 Microbial cores have been studied across holobionts (Ainsworth *et al.* 2015; Burke *et al.*  
465 2011; Schmitt *et al.* 2012; Shade & Handelsman 2012). Characterizing the core microbiota of  
466 a host, particularly over a large spatial or temporal scale (Shade & Handelsman 2012),  
467 provides an opportunity to detect patterns of stability and generality within a holobiont. After  
468 Bonthond *et al.* (2020) characterized a spatial core of epi- and endophytes within  
469 *G. vermiculophylla*, by sampling different populations of the host across its distribution range,  
470 the present work builds forward on this by characterizing temporal cores.

471 To identify core taxa of *G. vermiculophylla*, the present study utilized two compositional  
472 approaches (Shade & Handelsman 2012), resolving core OTUs based on statistically  
473 significant differential abundances. Both approaches corroborate our hypotheses that the  
474 *G. vermiculophylla* holobiont harbors prokaryotic taxa with strong temporal consistency, either  
475 associated permanently (Fig. 5A, D) or recurrently in summer (Fig. 5B, E) or winter (Fig. 5C,  
476 F).

477 Jointly, the spatial and temporal cores of Bonthond *et al.* (2020) and this study provide an  
478 elaborate, and to our knowledge unprecedented, impression of the core microbiota within a  
479 seaweed holobiont. A subset of 32 OTUs of the permanent mGLM-core was also identified as  
480 part of the spatial core in Bonthond *et al.* (2020). This set of OTUs is thus both geographically  
481 and temporally highly conserved, and represents a core that appears to be unconditionally  
482 present within this seaweed holobiont. In addition, 37 summer core OTUs and 50 winter core  
483 OTUs were also identified as spatial core OTUs in the previous study. While their presence in  
484 the *G. vermiculophylla* holobiont is season specific, they are also spatially and temporally  
485 consistent holobiont members.

486 Each of these taxa is of special interest, as their prevalent signal is unlikely coincidental.  
487 Perhaps most striking is the unclassified Alphaproteobacterial OTU (OTU12), which  
488 occurrence is 100% in both studies and whose poorly resolved identity may also indicate that  
489 the microbe is highly host-specific, and is difficult to isolate individually. Similarly, a member of  
490 the genus *Ahrensia* (OTU23), was present in 100% and > 99% of all samples in the spatial  
491 and present study, respectively. In addition to being identified as core spatial endophyte, both  
492 mGLM and LEfSe approaches resolved the *Ahrensia* OTU as permanent core member,  
493 implying a consistent presence of the holobiont.

494 The presence of a *Maribacter* core OTUs could hint at a host-microbe relationship within  
495 the *G. vermiculophylla* holobiont, similar to the chlorophyte *Ulva*, in which this bacterium plays  
496 a regulatory role in host morphogenesis (Weiss *et al.* 2017). Furthermore, the summer core  
497 also included the cyanobacterial OTU (OTU1), classified to *Pleurocapsa*, that was the most  
498 abundant OTU in the spatial study of Bonthond *et al.* (2020) and which was there found to be  
499 part of both epi- and endophytic cores. A closely related OTU, (OTU7, also classified to  
500 *Pleurocapsa*), also identified as spatial core endophyte and one of the most abundant OTUs  
501 in Bonthond *et al.* (2020), was here resolved as permanent core member. These  
502 cyanobacterial *Pleurocapsa* OTUs, are closely related to *Waterburya agarophytonicola*, which  
503 was isolated from the same host and has the genomic potential to synthesize various vitamins,

504 including cobalamin (vitamin B<sub>12</sub>) for which *G. vermiculophylla* is auxotroph (Bonthond *et al.*  
505 2021b). Such cyanobacterial core members may thus potentially play a role in vitamin  
506 acquisition for the seaweed host.

507 Noteworthy is the detection of three *Granulosicoccus* OTUs as part of the winter core (OTUs  
508 2, 41 and 97), of which two were resolved as spatial core endophytes in Bonthond *et al.* (2020).  
509 The genus *Granulosicoccus* is considered to be a seaweed generalist and is often reported as  
510 core symbiont (Aires *et al.* 2023; Park *et al.* 2022). Metagenomic evidence from the Kelp  
511 *Nereocystis luetkeana* suggested that associated *Granulosicoccus* have diverse energy  
512 metabolism, but are incapable of autotrophic carbon fixation, which may indicate they obtain  
513 organic carbon from their seaweed host (Weigel *et al.* 2022). Moreover, Weigel *et al.* (2022)  
514 also found that *Granulosicoccus* have all genes necessary to synthesize cobalamin, which  
515 makes them another candidate vitamin source for the auxotrophic host *G. vermiculophylla*.  
516

517

## 518 **CONCLUSION**

519 Altogether, this study provides to the best of our knowledge one of the most detailed studies  
520 on seasonality in microbiota within a seaweed holobiont, with repeating a bi-monthly sampling  
521 over three years. Epibiota associated with *Gracilaria vermiculophylla* are dynamic, and  
522 seasonality drives much of this temporal variation in diversity and composition. These seasonal  
523 differences are likely linked to environmental conditions such as salinity and temperature,  
524 which fluctuate strongly throughout the year, especially in the shallow and intertidal habitats  
525 where this seaweed typically occurs. Despite strong compositional differences between North  
526 and Baltic Sea populations, similar cyclic patterns were resolved between the two populations,  
527 which reflects that despite strong differences between populations, they experience similar  
528 seasonal succession cycles, and which are thus likely natural to *G. vermiculophylla* holobionts.  
529 These succession cycles entail functional changes, as the cyclic trend was also evident in  
530 predicted functional composition. In contrast, differences between populations were minimal  
531 in terms of functional composition, which suggests that unlike the spatial shifts, seasonal  
532 changes are more functional. Based on this we posit that spatial variability in microbial  
533 composition within the *G. vermiculophylla* holobiont is more redundant than seasonal  
534 variability, because essential microbial functions can be obtained from a wide range of  
535 microbes.

536 While epibiota vary in space and time, we resolved 32 OTUs, which are permanent core  
537 members in this study and part of the spatial core characterized in earlier work of Bonthond *et al.*  
538 (2020). Therewith, this study demonstrates that certain microbial taxa are perpetual within  
539 the holobiont and are season and geography independent. This spatial and temporal core  
540 presents a subset of candidate microorganisms that may play important roles in host  
541 functioning and which merits future attention.

542

543

## 544 **AUTHOR CONTRIBUTIONS**

545 CMM, FW and GB conceptualized the study. Field collections were conducted by CMM,  
546 FW, LD and GB. CMM, FW, LD, MG, SK and GB conducted laboratory work. CMM, FW and  
547 GB processed data. CMM, FW and GB conducted the formal analysis. CMM, FW and GB  
548 drafted the manuscript. All authors contributed to writing and revising the manuscript.

549

550

## 551 **ACKNOWLEDGEMENTS**

552 This study was funded by the Deutsche Forschungsgemeinschaft (DFG), through a grant  
553 awarded to FW (DFG grant number WE2700/5-1). The authors are grateful to Nabila Elarbi,  
554 Barbora Burýšková and Fatiha Kalam Nisa for support during fieldwork and to the Deutsche  
555 Bundesamt für Seeschifffahrt und Hydrographie (BSH) for kindly providing temperature data.

556  
557

#### 558 **CONFLICT OF INTEREST STATEMENT**

559 The authors declare there is no conflict of interest.

560  
561

#### 562 **DATA AVAILABILITY STATEMENT**

563 The raw de-multiplexed V4-16S rDNA gene amplicon reads and associated metadata are  
564 available from the SRA database under the Bioproject accession number PRJNA1155875.  
565 Other data and R-scripts for analyses are available on GitHub at  
566 [https://github.com/gbonthond/Seasonality\\_seaweed\\_holobiont](https://github.com/gbonthond/Seasonality_seaweed_holobiont).

567  
568  
569

570 **REFERENCES**

- 571
- 572 Ainsworth, T., Krause, L., Bridge, T., Torda, G., Raina, J.-B., Zakrzewski, M., *et al.*  
573 (2015). The coral core microbiome identifies rare bacterial taxa as ubiquitous  
574 endosymbionts. *The ISME Journal*, 9, 2261–2274.
- 575 Aires, T., Kläui, A. & Engelen, A. (2023). Regional microbiome differentiation of the  
576 invasive *Sargassum muticum* (Fucales, Phaeophyceae) follows the generalist  
577 host hypothesis across the North East Atlantic. *European Journal of Phycology*,  
578 58, 268–283.
- 579 Bellorin, A.M., Oliveira, M.C. & Oliveira, E.C. (2004). *Gracilaria vermiculophylla*: A  
580 western Pacific species of Gracilariaceae (Rhodophyta) first recorded from the  
581 eastern Pacific. *Phycological Res*, 52, 69–79.
- 582 Bengtsson, M., Sjøtun, K. & Øvreås, L. (2010). Seasonal dynamics of bacterial biofilms  
583 on the kelp *Laminaria hyperborea*. *Aquat. Microb. Ecol.*, 60, 71–83.
- 584 Benincà, E., Ballantine, B., Ellner, S.P. & Huisman, J. (2015). Species fluctuations  
585 sustained by a cyclic succession at the edge of chaos. *Proc. Natl. Acad. Sci.*  
586 *U.S.A.*, 112, 6389–6394.
- 587 Bonthond, G., Barilo, A., Allen, R.J., Cunliffe, M. & Krueger-Hadfield, S.A. (2022).  
588 Fungal endophytes vary by species, tissue type, and life cycle stage in intertidal  
589 macroalgae. *J. Phycol.*, 58, 330–342.
- 590 Bonthond, G., Bayer, T., Krueger-Hadfield, S.A., Barboza, F.R., Nakaoka, M., Valero,  
591 M., *et al.* (2020). How do microbiota associated with an invasive seaweed vary  
592 across scales? *Mol Ecol*, 29, 2094–2108.
- 593 Bonthond, G., Bayer, T., Krueger-Hadfield, S.A., Stärck, N., Wang, G., Nakaoka, M.,  
594 *et al.* (2021a). The role of host promiscuity in the invasion process of a seaweed  
595 holobiont. *ISME J*, 15, 1668–1679.
- 596 Bonthond, G., Neu, A., Bayer, T., Krueger-Hadfield, S.A., Künzel, S. & Weinberger, F.  
597 (2023). Non-native hosts of an invasive seaweed holobiont have more stable  
598 microbial communities compared to native hosts in response to thermal stress.  
599 *Ecology and Evolution*, 13.
- 600 Bonthond, G., Shalygin, S., Bayer, T. & Weinberger, F. (2021b). Draft genome and  
601 description of *Waterburya agarophytonicola* gen. nov. sp. nov. (Pleurocapsales,  
602 Cyanobacteria): a seaweed symbiont. *Antonie van Leeuwenhoek*, 114, 2189–  
603 2203.
- 604 Burgunter-Delamare, B., Rousvoal, S., Legeay, E., Tanguy, G., Fredriksen, S., Boyen,  
605 C., *et al.* (2023). The *Saccharina latissima* microbiome: Effects of region,  
606 season, and physiology. *Front. Microbiol.*, 13, 1050939.
- 607 Burke, C., Steinberg, P., Rusch, D., Kjelleberg, S. & Thomas, T. (2011). Bacterial  
608 community assembly based on functional genes rather than species. *Proc. Natl.*  
609 *Acad. Sci. U.S.A.*, 108, 14288–14293.
- 610 Chao, A., Gotelli, N.J., Hsieh, T.C., Sander, E.L., Ma, K.H., Colwell, R.K., *et al.* (2014).  
611 Rarefaction and extrapolation with Hill numbers: a framework for sampling and  
612 estimation in species diversity studies. *Ecological Monographs*, 84, 45–67.
- 613 Clarke, A. & Fraser, K.P.P. (2004). Why Does Metabolism Scale with Temperature?  
614 *Functional Ecology*, 18, 243–251.
- 615 Douglas, G.M., Maffei, V.J., Zaneveld, J.R., Yurgel, S.N., Brown, J.R., Taylor, C.M., *et*  
616 *al.* (2020). PICRUSt2 for prediction of metagenome functions. *Nat Biotechnol*,  
617 38, 685–688.
- 618 Doyle, J.J. & Doyle, J.L. (1987). A rapid DNA isolation procedure for small quantities  
619 of fresh leaf tissue. *Phytochemical bulletin*.

- 620 Düsedau, L., Ren, Y., Hou, M., Wahl, M., Hu, Z.-M., Wang, G., *et al.* (2023). Elevated  
621 Temperature-Induced Epimicrobiome Shifts in an Invasive Seaweed *Gracilaria*  
622 *vermiculophylla*. *Microorganisms*, 11, 599.
- 623 Egan, S., Harder, T., Burke, C., Steinberg, P., Kjelleberg, S. & Thomas, T. (2013). The  
624 seaweed holobiont: understanding seaweed–bacteria interactions. *FEMS*  
625 *Microbiol Rev*, 37, 462–476.
- 626 Federal Maritime and Hydrographic Agency (BSH). (2023). BSH sea-surface  
627 temperature analysis North Sea.
- 628 Ferguson, L.V., Dhakal, P., Lebenzon, J.E., Heinrichs, D.E., Bucking, C. & Sinclair,  
629 B.J. (2018). Seasonal shifts in the insect gut microbiome are concurrent with  
630 changes in cold tolerance and immunity. *Functional Ecology*, 32, 2357–2368.
- 631 Ficetola, G.F., Miaud, C., Pompanon, F. & Taberlet, P. (2008). Species detection using  
632 environmental DNA from water samples. *Biol. Lett.*, 4, 423–425.
- 633 Freshwater, W.D., Montgomery, F., Greene, J.K., Hamner, R.M., Williams, M. &  
634 Whitfield, P.E. (2006). Distribution and Identification of an Invasive *Gracilaria*  
635 Species that is Hampering Commercial Fishing Operations in Southeastern  
636 North Carolina, USA. *Biol Invasions*, 8, 631–637.
- 637 Fuhrman, J.A., Cram, J.A. & Needham, D.M. (2015). Marine microbial community  
638 dynamics and their ecological interpretation. *Nat Rev Microbiol*, 13, 133–146.
- 639 Gilbert, J.A., Steele, J.A., Caporaso, J.G., Steinbrück, L., Reeder, J., Temperton, B.,  
640 *et al.* (2012). Defining seasonal marine microbial community dynamics. *The*  
641 *ISME Journal*, 6, 298–308.
- 642 Gillooly, J.F., Brown, J.H., West, G.B., Savage, V.M. & Charnov, E.L. (2001). Effects  
643 of Size and Temperature on Metabolic Rate. *Science*, 293, 2248–2251.
- 644 Gobbi, A., Kyrkou, I., Filippi, E., Ellegaard-Jensen, L. & Hansen, L.H. (2020). Seasonal  
645 epiphytic microbial dynamics on grapevine leaves under biocontrol and copper  
646 fungicide treatments. *Sci Rep*, 10, 681.
- 647 Gohl, D.M., Vangay, P., Garbe, J., MacLean, A., Hauge, A., Becker, A., *et al.* (2016).  
648 Systematic improvement of amplicon marker gene methods for increased  
649 accuracy in microbiome studies. *Nat Biotechnol*, 34, 942–949.
- 650 Hsieh, T.C., Ma, K.H. & Chao, A. (2016). iNEXT: an R package for rarefaction and  
651 extrapolation of species diversity ( Hill numbers). *Methods Ecol Evol*, 7, 1451–  
652 1456.
- 653 Hurlbert, S.H. (1971). The Nonconcept of Species Diversity: A Critique and Alternative  
654 Parameters. *Ecology*, 52, 577–586.
- 655 Kanehisa, M., Goto, S., Sato, Y., Kawashima, M., Furumichi, M. & Tanabe, M. (2014).  
656 Data, information, knowledge and principle: back to metabolism in KEGG. *Nucl.*  
657 *Acids Res.*, 42, D199–D205.
- 658 Kim, S.Y., Weinberger, F. & Boo, S.M. (2010). Genetic data hint at a common donor  
659 region for invasive Atlantic and Pacific populations of *Gracilaria vermiculophylla*  
660 (*Gracilariales*, *Rhodophyta*). *Journal of Phycology*, 46, 1346–1349.
- 661 Klindworth, A., Pruesse, E., Schweer, T., Peplies, J., Quast, C., Horn, M., *et al.* (2013).  
662 Evaluation of general 16S ribosomal RNA gene PCR primers for classical and  
663 next-generation sequencing-based diversity studies. *Nucleic Acids Res*, 41, e1–  
664 e1.
- 665 Korlević, M., Markovski, M., Zhao, Z., Herndl, G.J. & Najdek, M. (2021). Seasonal  
666 Dynamics of Epiphytic Microbial Communities on Marine Macrophyte Surfaces.  
667 *Front. Microbiol.*, 12, 671342.
- 668 Krueger-Hadfield, S.A., Byers, J.E., Bonthond, G., Terada, R., Weinberger, F. & Sotka,  
669 E.E. (2021). Intraspecific diversity and genetic structure in the widespread  
670 macroalga *Agarophyton vermiculophyllum*. *J. Phycol.*, 57, 1403–1410.

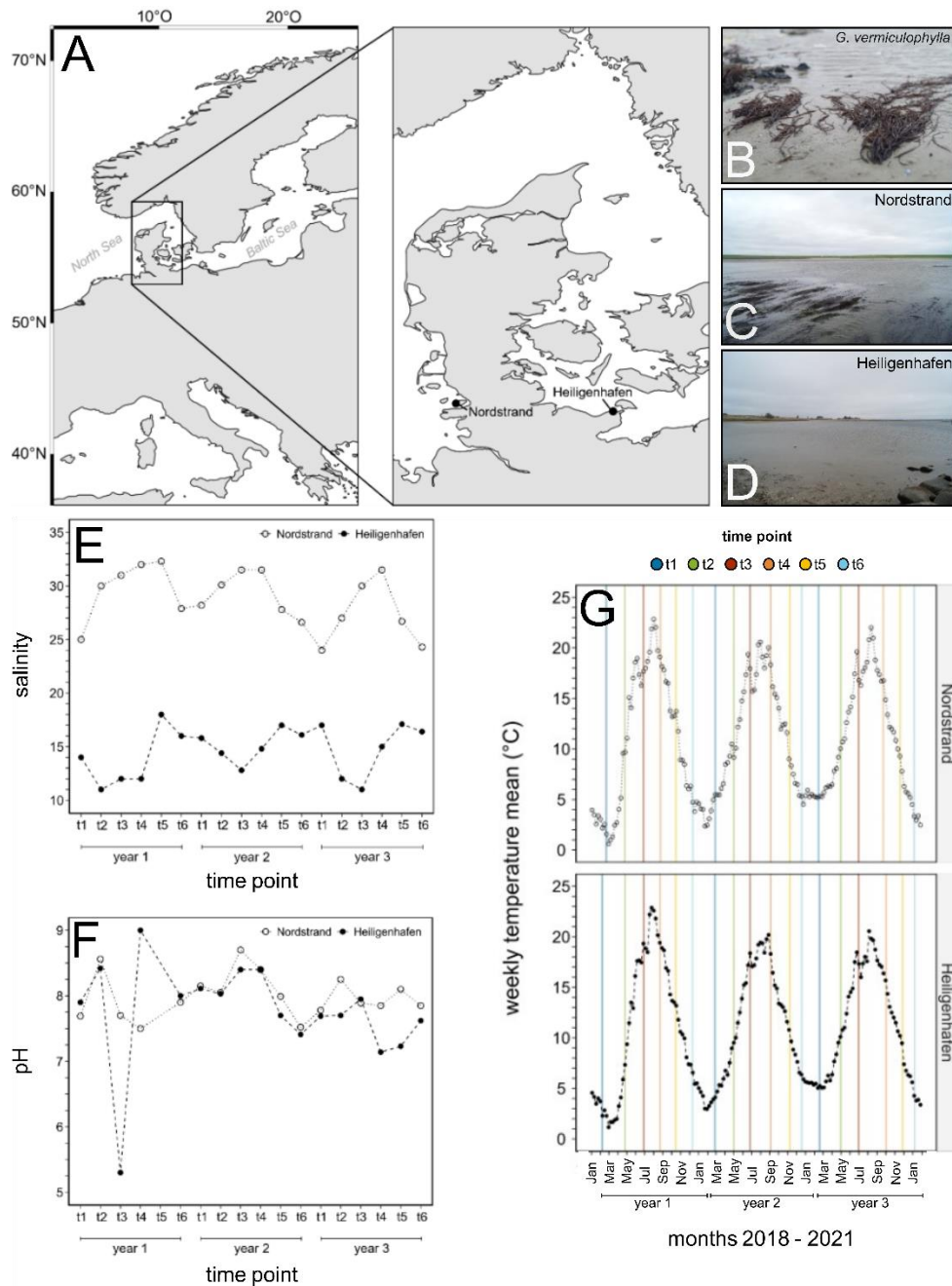


- 671 Krueger-Hadfield, S.A., Kollars, N.M., Strand, A.E., Byers, J.E., Shainker, S.J., Terada,  
672 R., *et al.* (2017). Genetic identification of source and likely vector of a  
673 widespread marine invader. *Ecology and Evolution*, 7, 4432–4447.
- 674 Lachnit, T., Blümel, M., Imhoff, J. & Wahl, M. (2009). Specific epibacterial communities  
675 on macroalgae: phylogeny matters more than habitat. *Aquat. Biol.*, 5, 181–186.
- 676 Lachnit, T., Meske, D., Wahl, M., Harder, T. & Schmitz, R. (2011). Epibacterial  
677 community patterns on marine macroalgae are host-specific but temporally  
678 variable. *Environmental Microbiology*, 13, 655–665.
- 679 Lemay, M.A., Chen, M.Y., Mazel, F., Hind, K.R., Starko, S., Keeling, P.J., *et al.* (2021).  
680 Morphological complexity affects the diversity of marine microbiomes. *The*  
681 *ISME Journal*, 15, 1372–1386.
- 682 Lemay, M.A., Martone, P.T., Hind, K.R., Lindstrom, S.C. & Wegener Parfrey, L. (2018).  
683 Alternate life history phases of a common seaweed have distinct microbial  
684 surface communities. *Molecular Ecology*, 27, 3555–3568.
- 685 Lenth, R.V. (2022). emmeans: estimated marginal means, aka least-squares means.
- 686 Li, J., Weinberger, F., Saha, M., Majzoub, M.E. & Egan, S. (2022). Cross-Host  
687 Protection of Marine Bacteria Against Macroalgal Disease. *Microb Ecol*, 84,  
688 1288–1293.
- 689 Lisovski, S., Ramenofsky, M. & Wingfield, J.C. (2017). Defining the Degree of  
690 Seasonality and its Significance for Future Research. *Integrative and*  
691 *Comparative Biology*, 57, 934–942.
- 692 Liu, X., Bogaert, K., Engelen, A.H., Leliaert, F., Roleda, M.Y. & De Clerck, O. (2017).  
693 Seaweed reproductive biology: environmental and genetic controls. *Botanica*  
694 *Marina*, 60.
- 695 Longford, S.R., Campbell, A.H., Nielsen, S., Case, R.J., Kjelleberg, S. & Steinberg,  
696 P.D. (2019). Interactions within the microbiome alter microbial interactions with  
697 host chemical defences and affect disease in a marine holobiont. *Sci Rep*, 9,  
698 1363.
- 699 Mancuso, F.P., D'Hondt, S., Willems, A., Airoidi, L. & De Clerck, O. (2016). Diversity  
700 and Temporal Dynamics of the Epiphytic Bacterial Communities Associated  
701 with the Canopy-Forming Seaweed *Cystoseira compressa* (Esper) Gerloff and  
702 Nizamuddin. *Front. Microbiol.*, 7.
- 703 McGlinn, D.J., Xiao, X., May, F., Gotelli, N.J., Engel, T., Blowes, S.A., *et al.* (2019).  
704 Measurement of Biodiversity (MoB): A method to separate the scale-dependent  
705 effects of species abundance distribution, density, and aggregation on diversity  
706 change. *Methods Ecol Evol*, 10, 258–269.
- 707 Oksanen, J. (2010). Vegan: community ecology package. [http://vegan.r-forge.r-](http://vegan.r-forge.r-project.org/)  
708 [project.org/](http://vegan.r-forge.r-project.org/).
- 709 Paix, B., Carriot, N., Barry-Martinet, R., Greff, S., Misson, B., Briand, J.-F., *et al.* (2020).  
710 A Multi-Omics Analysis Suggests Links Between the Differentiated Surface  
711 Metabolome and Epiphytic Microbiota Along the Thallus of a Mediterranean  
712 Seaweed Holobiont. *Front. Microbiol.*, 11, 494.
- 713 Paix, B., Othmani, A., Debroas, D., Culioli, G. & Briand, J. (2019). Temporal covariation  
714 of epibacterial community and surface metabolome in the Mediterranean  
715 seaweed holobiont *TAONIA ATOMARIA*. *Environmental Microbiology*, 21, 3346–  
716 3363.
- 717 Park, J., Davis, K., Lajoie, G. & Parfrey, L.W. (2022). Alternative approaches to identify  
718 core bacteria in *Fucus distichus* microbiome and assess their distribution and  
719 host-specificity. *Environmental Microbiome*, 17, 55.

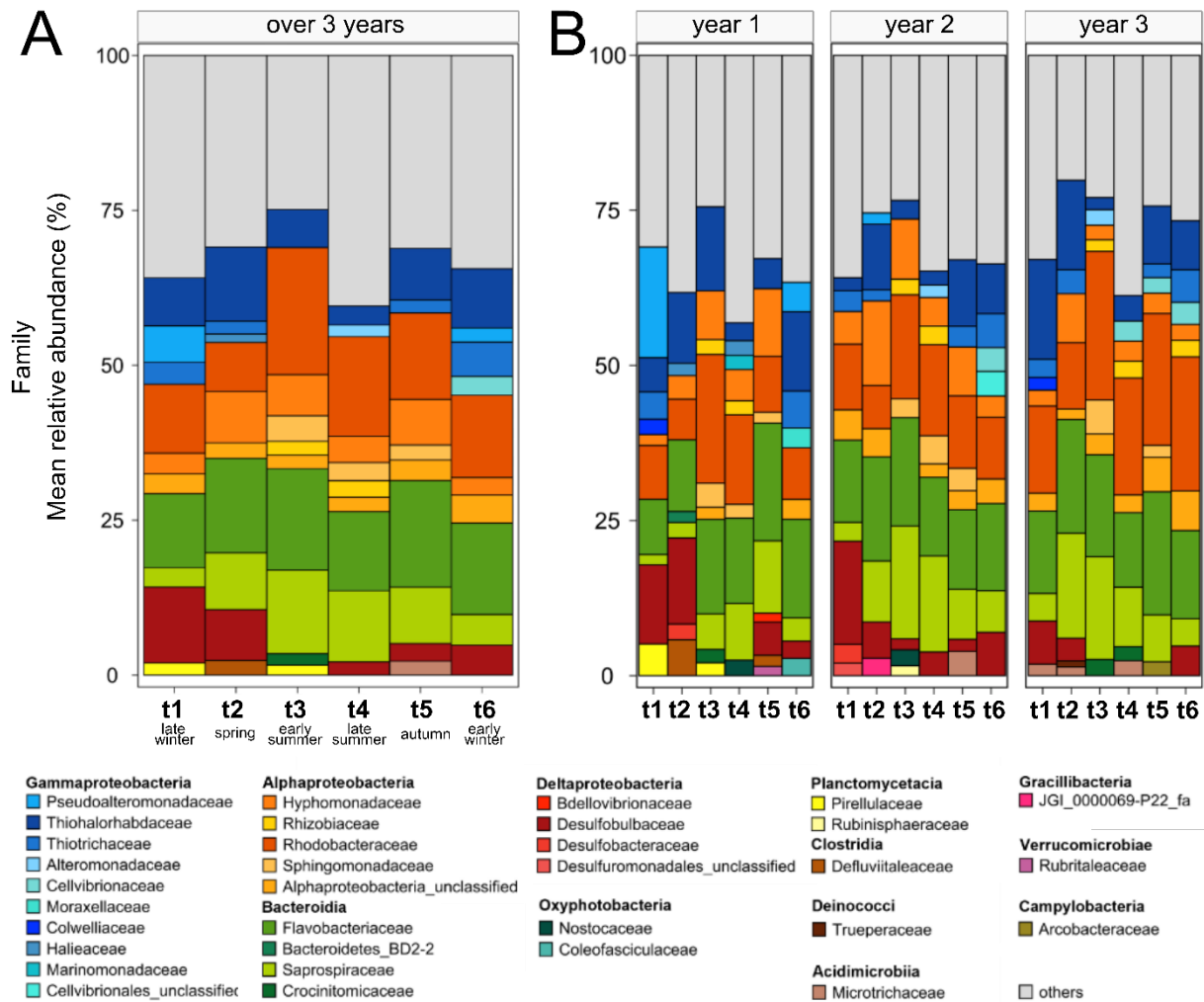
- 720 Quast, C., Pruesse, E., Yilmaz, P., Gerken, J., Schweer, T., Yarza, P., *et al.* (2013).  
721 The SILVA ribosomal RNA gene database project: improved data processing  
722 and web-based tools. *Nucleic Acids Res*, 41, D590–D596.
- 723 Rao, D., Webb, J.S., Holmström, C., Case, R., Low, A., Steinberg, P., *et al.* (2007).  
724 Low Densities of Epiphytic Bacteria from the Marine Alga *Ulva australis* Inhibit  
725 Settlement of Fouling Organisms. *Appl Environ Microbiol*, 73, 7844–7852.
- 726 Risely, A., Wilhelm, K., Clutton-Brock, T., Manser, M.B. & Sommer, S. (2021). Diurnal  
727 oscillations in gut bacterial load and composition eclipse seasonal and lifetime  
728 dynamics in wild meerkats. *Nat Commun*, 12, 6017.
- 729 Rueness, J. (2005). Life history and molecular sequences of *Gracilaria vermiculophylla*  
730 (Gracilariales, Rhodophyta), a new introduction to European waters.  
731 *Phycologia*, 44, 120–128.
- 732 Saha, M. & Wahl, M. (2013). Seasonal variation in the antifouling defence of the  
733 temperate brown alga *Fucus vesiculosus*. *Biofouling*, 29, 661–668.
- 734 Saha, M. & Weinberger, F. (2019). Microbial “gardening” by a seaweed holobiont:  
735 surface metabolites attract protective and deter pathogenic epibacterial  
736 settlement. *Journal of Ecology*, 107, 2255–2265.
- 737 Schloss, P.D., Westcott, S.L., Ryabin, T., Hall, J.R., Hartmann, M., Hollister, E.B., *et*  
738 *al.* (2009). Introducing mothur: Open-Source, Platform-Independent,  
739 Community-Supported Software for Describing and Comparing Microbial  
740 Communities. *Appl Environ Microbiol*, 75, 7537–7541.
- 741 Schmitt, S., Tsai, P., Bell, J., Fromont, J., Ilan, M., Lindquist, N., *et al.* (2012).  
742 Assessing the complex sponge microbiota: core, variable and species-specific  
743 bacterial communities in marine sponges. *The ISME Journal*, 6, 564–576.
- 744 Segata, N., Izard, J., Waldron, L., Gevers, D., Miropolsky, L., Garrett, W.S., *et al.*  
745 (2011). Metagenomic biomarker discovery and explanation. *Genome Biol*, 12,  
746 R60.
- 747 Shade, A. & Handelsman, J. (2012). Beyond the Venn diagram: the hunt for a core  
748 microbiome. *Environmental Microbiology*, 14, 4–12.
- 749 Sharp, K.H., Pratte, Z.A., Kerwin, A.H., Rotjan, R.D. & Stewart, F.J. (2017). Season,  
750 but not symbiont state, drives microbiome structure in the temperate coral  
751 *Astrangia poculata*. *Microbiome*, 5, 120.
- 752 Sovacool, K.L., Westcott, S.L., Mumphrey, M.B., Dotson, G.A. & Schloss, P.D. (2022).  
753 OptiFit: an Improved Method for Fitting Amplicon Sequences to Existing OTUs.  
754 *mSphere*, 7, e00916-21.
- 755 Stanley, S.J. (1992). Observations on the seasonal occurrence of marine endophytic  
756 and parasitic fungi. *Can. J. Bot.*, 70, 2089–2096.
- 757 Stratil, S.B., Neulinger, S.C., Knecht, H., Friedrichs, A.K. & Wahl, M. (2013).  
758 Temperature-driven shifts in the epibiotic bacterial community composition of  
759 the brown macroalga *Fucus vesiculosus*. *MicrobiologyOpen*, 2, 338–349.
- 760 Stratil, S.B., Neulinger, S.C., Knecht, H., Friedrichs, A.K. & Wahl, M. (2014). Salinity  
761 affects compositional traits of epibacterial communities on the brown macroalga  
762 *Fucus vesiculosus*. *FEMS Microbiol Ecol*, 88, 272–279.
- 763 Thomsen, M. (2007). *Gracilaria vermiculophylla* (Ohmi) Papenfuss, 1967  
764 (Rhodophyta, Gracilariaceae) in northern Europe, with emphasis on Danish  
765 conditions, and what to expect in the future. *Al*, 2, 83–94.
- 766 Thomsen, M.S., Gurgel, C.F.D., Fredericq, S. & McGlathery, K.J. (2006). *Gracilaria*  
767 *vermiculophylla* (Rhodophyta, Gracilariales) in Hog Island Bay, Virginia: A  
768 cryptic alien and invasive macroalga and taxonomic correction. *Journal of*  
769 *Phycology*, 42, 139–141.

- 770 Tujula, N.A., Crocetti, G.R., Burke, C., Thomas, T., Holmström, C. & Kjelleberg, S.  
771 (2010). Variability and abundance of the epiphytic bacterial community  
772 associated with a green marine *Ulvacean* alga. *The ISME Journal*, 4, 301–311.
- 773 Van Der Loos, L.M., D'hondt, S., Engelen, A.H., Pavia, H., Toth, G.B., Willems, A., *et*  
774 *al.* (2023). Salinity and host drive *Ulva* -associated bacterial communities across  
775 the Atlantic–Baltic Sea gradient. *Molecular Ecology*, 32, 6260–6277.
- 776 Van Der Loos, L.M., Eriksson, B.K. & Falcão Salles, J. (2019). The Macroalgal  
777 Holobiont in a Changing Sea. *Trends in Microbiology*, 27, 635–650.
- 778 Wahl, M., Goecke, F., Labes, A., Dobretsov, S. & Weinberger, F. (2012). The second  
779 skin: ecological role of epibiotic biofilms on marine organisms. *Frontiers in*  
780 *microbiology*, 3, 292.
- 781 Wang, S., Weinberger, F. & Lenz, M. (2018). Fluctuations in the strength of chemical  
782 antifouling defenses in a red macroalga in response to variations in epibiont  
783 colonization pressure. *Mar Biol*, 165, 107.
- 784 Wang, Y., Naumann, U., Wright, S.T. & Warton, D.I. (2012). mvabund - an R package  
785 for model-based analysis of multivariate abundance data: *The mvabund R*  
786 *package*. *Methods in Ecology and Evolution*, 3, 471–474.
- 787 Weigel, B.L., Miranda, K.K., Fogarty, E.C., Watson, A.R. & Pfister, C.A. (2022).  
788 Functional Insights into the Kelp Microbiome from Metagenome-Assembled  
789 Genomes. *mSystems*, 7, e01422-21.
- 790 Weinberger, F., Beltran, J., Correa, J.A., Lion, U., Pohnert, G., Kumar, N., *et al.* (2007).  
791 Spore release in *Acrochaetium* sp. (Rhodophyta) is bacterially controlled.  
792 *Journal of Phycology*, 43, 235–241.
- 793 Weinberger, F., Buchholz, B., Karez, R. & Wahl, M. (2008). The invasive red alga  
794 *Gracilaria vermiculophylla* in the Baltic Sea: adaptation to brackish water may  
795 compensate for light limitation. *Aquat. Biol.*, 3, 251–264.
- 796 Weiss, A., Costa, R. & Wichard, T. (2017). Morphogenesis of *Ulva mutabilis*  
797 (Chlorophyta) induced by *Maribacter* species (Bacteroidetes,  
798 Flavobacteriaceae). *Botanica Marina*, 60.
- 799 White, E.R. & Hastings, A. (2020). Seasonality in ecology: Progress and prospects in  
800 theory. *Ecological Complexity*, 44, 100867.
- 801  
802  
803  
804

805 **FIGURES**  
806



807  
808 **Figure 1.** Overview of the two collection sites Nordstrand (North Sea) and Heiligenhafen (Baltic  
809 Sea), where the bi-monthly sampling of *Gracilaria vermiculophylla* was carried out, and  
810 environmental parameters during the three-year time period. (A) Map showing the two  
811 collection sites. (B) Habitus of *Gracilaria vermiculophylla*. (C) North Sea population found at  
812 Nordstrand, (D) Baltic Sea population found at Heiligenhafen. (E) Salinity and (F) pH measured  
813 during the field sampling. (G) The weekly water temperature (°C) obtained from nearby  
814 measuring stations, with vertical lines depicting the exact collection time points. Temperature  
815 data provided by the German Federal Maritime and Hydrographic Agency (BSH, 2023).  
816



817

818

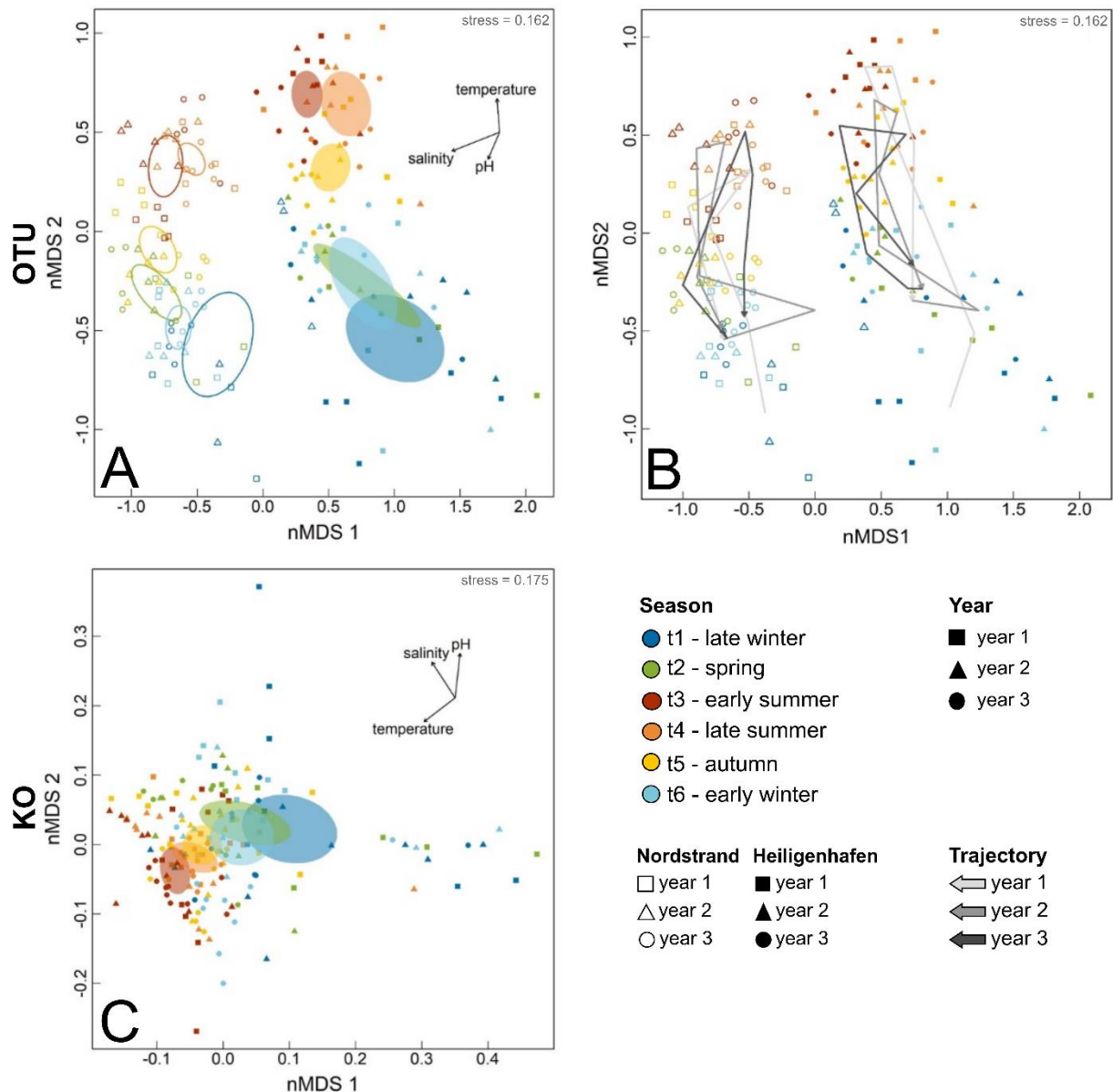
819 **Figure 2.** Microbial community composition of the ten most abundant families associated with

820 the surface of the red seaweed *Gracilaria vermiculophylla*, at **(A)** season time points averaged

821 over populations and years, and **(B)** season time points for each year averaged over

822 populations. Shown is the mean relative abundance in percent (%).

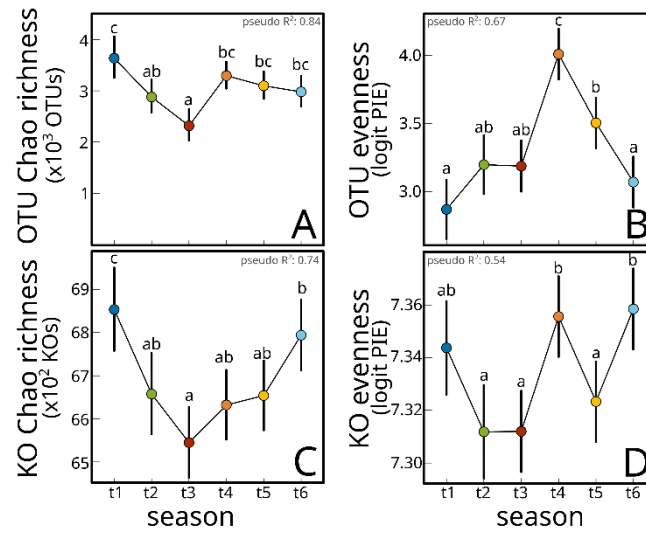
822



823

824 **Figure 3.** Nonmetric-multidimensional scaling (nMDS) of the microbial taxonomic (A, B) and  
 825 functional (C) diversity associated with the red seaweed *Gracilaria vermiculophylla*. The  
 826 season time points are pooled over populations and years and are displayed with a unique  
 827 color coding as follows: t1 (late winter) in dark blue, t2 (spring) in green, t3 (early summer) in  
 828 red, t4 (late summer) in orange, t5 (autumn) in yellow, and t6 (early winter) in light blue. The  
 829 corresponding ellipses are represented with a 95% confidence interval. The years can be  
 830 differentiated by their shape i.e., a square for year 1, triangle for year 2 and dot for year 3.  
 831 Additionally, the abiotic factors temperature, salinity, and pH are plotted. The stress value is  
 832 given in the upper right corner. The taxonomic (based on OTUs) and functional (based on  
 833 predicted KOs) diversity shown is based on rarefied data including solely algal samples.

834

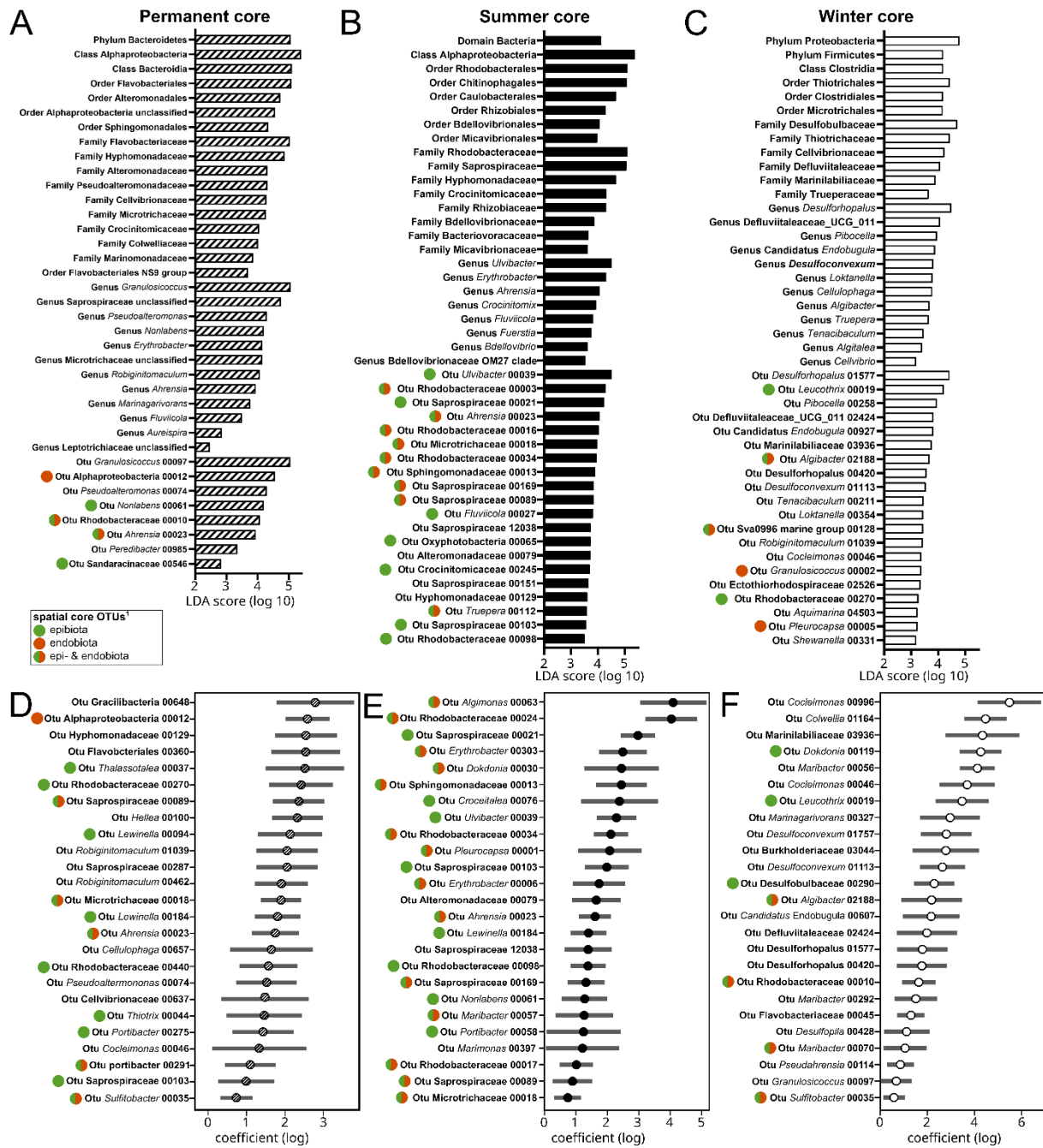


835

836 **Figure 4.** Estimated means of Chao OTU richness (A), OTU evenness (B), Chao KO richness  
837 (C) and KO evenness (D) from GLMs fitted on two diversity measures among the six season  
838 time points. Error bars show 95% confidence intervals. The Cox and Snell pseudo R<sup>2</sup> is given  
839 in each corner of the respective plot. Significantly different time points within pair-wise  
840 comparisons in the post-hoc analysis are indicated by small letters.

841

842



843  
 844 **Figure 5.** Permanent (A, D), summer (B, E) and winter (C, F) core epibiota associated with  
 845 the rodophyte *Gracilaria vermiculophylla*. (A-C) Core taxa at different taxonomic levels  
 846 detected with LEFse. (D-F) Core OTUs detected using mGLMs. Only the top 25 most abundant  
 847 core OTUs are shown. <sup>(1)</sup> Green, red and green-red circles in front of the taxon labels indicate  
 848 OTUs identified as spatial core OTUs in Bonthond *et al.* (2020).  
 849



850 **SUPPORTING INFORMATION**

851

852 **Table S1.** PERMANOVA community composition all substrates

853 **Table S2.** PERMANOVA community composition on only algal substrate

854 **Table S3.** PERMANOVA predicted functional composition on only algal substrate

855 **Table S4. (A)** ANOVA table for asymptotic richness ( $S_{\text{Chao}}$ ) based on OTUs and KOs. **(B)**

856 Post-hoc pair-wise comparisons within the factor season (t1 – t6) for asymptotic richness

857 ( $S_{\text{Chao}}$ ) based on OTUs and KOs

858 **Table S5. (A)** ANOVA table for evenness (Probability of Interspecific Encounter) based on

859 OTUs and KOs. **(B)** Post-hoc pair-wise comparisons within the factor season (t1 – t6) for for

860 evenness (Probability of Interspecific Encounter) based on OTUs and KOs.

861 **Table S6.** Epiphytic cores

862 **Table S7.** Higher taxonomic rank cores

863

864 **Figure S1.** Stacked bar plots showing community composition by substrate

865 **Figure S2.** Stacked bar plots showing community composition by population

866 **Figure S3.** Stacked bar plots showing community composition by population, year, and

867 collection event

868 **Figure S4.** nMDS with algal, water, and sediment samples

869